Infusion of Presynthesized Iridium Nanocrystals into Mesoporous Silica for High Catalyst Activity

Gaurav Gupta, Cynthia A. Stowell, Mehul N. Patel, Xiaoxia Gao, Miguel J. Yacaman, Brian A. Korgel,* and Keith P. Johnston*

Department of Chemical Engineering and Texas Materials Institute, Center for Nano- and Molecular Science and Technology, The University of Texas, Austin, Texas 78712-1062

Received July 18, 2006. Revised Manuscript Received October 3, 2006

Traditionally, finely dispersed metal catalysts have been formed by reduction of precursors within mesoporous supports. A new concept for designing catalysts with enhanced activities and selectivities is to infuse presynthesized nanocrystals with well-defined morphologies into ordered mesoporous materials. The decoupling of nanocrystal synthesis and infusion provides exquisite control of the nanocrystal size, morphology, and dispersibility within the pores. A dispersion of iridium nanocrystals was infused into mesoporous silica by expanding the solvent toluene with supercritical CO_2. To achieve high nanocrystal loadings, up to 1.3 wt %, we tuned the solvent quality to strengthen the interactions of the nanocrystals with the pore walls, but without precipitating the nanocrystals in the bulk solvent. Z-contrast STEM indicates conclusively that the iridium nanocrystals were located within the pores and not on the external silica surface. High catalytic activity was observed for 1-decene hydrogenation, which is consistent with a high degree of dispersion of the 4.5 nm nanocrystals throughout the pores, as observed by TEM. A maximum turnover frequency (TOF) of 16 s^{-1} was measured, which was higher than the initial TOF for homogeneous catalysis with the same nanocrystals in 1-decene. The iridium catalysts do not require pretreatment to remove the tetraoctylammonium bromide ligands to achieve activation, as the ligands bind weakly to the iridium surface. Consequently, the activity was not enhanced when calcined at 500 °C in nitrogen or when annealed in supercritical CO_2 at 275 bar. The ability to predesign nanocrystal morphology and surface properties prior to infusion into the mesoporous silica support offers novel opportunities for enhanced catalyst activity, stability, and reaction selectivity.

Introduction

In catalysis, substantial improvements in turnover rates and selectivities are possible with metal nanocrystals containing high concentrations of active surface sites.[1,2] Nanocrystal growth may be controlled in solution with stabilizing ligands to achieve specific size, crystallinity, shape, and surface properties.[3] The design of the surface sites on the nanocrystals may be guided by fundamental studies of reaction mechanisms on well-defined surfaces on single crystals.[4,5] Immobilization of the nanocrystals within the pores of a mesoporous support helps maintain high surface area by preventing coalescence of the nanocrystals during reaction.[6] The size of the mesopores may be designed to influence reaction selectivity and catalyst activity by limiting access to the nanocrystals for certain reactants and products as a function of their size. Finally, the immobilization on the support facilitates catalyst recovery and recycles.

Traditionally, supported catalysts are synthesized by precursor reduction,[6−8] ion exchange,[9,10] and chemical vapor/fluid deposition.[11−13] In these techniques, it is challenging to control the metal cluster size and surface morphology. One approach to metal nanocrystal encapsulation within a mesoporous support is to form the mesoporous structure in the presence of a dispersion of presynthesized nanocrystals.[14,15] In this technique, it can be difficult to achieve high loadings of dispersed nanocrystals within the pores. In addition, the presence of the particles can interfere with the synthesis of the desired pore structure and, conversely, the synthesis of the mesoporous material can change the morphology of the nanocrystals. For example, the ligands stabilizing the nanocrystals may desorb and adsorb onto the

* Corresponding author. Fax: 512-471-7060. Phone: 512-471-4617. E-mail: kpj@che.utexas.edu (K.P.J.); korgel@che.utexas.edu (B.A.K.).

(1) Scott, R. W. J.; Wilson, O. M.; Crooks, R. M. *J. Phys. Chem. B* **2005**, *109*, 692−704.
(2) Rolison, D. R. *Science* **2003**, *299*, 1698−1702.
(3) Kanaras, A. G.; Soennichsen, C.; Liu, H.; Alivisatos, A. P. *Nano Lett.* **2005**, *5*, 2164−2167.
(4) Farias, M. H.; Gellman, A. J.; Somorjai, G. A.; Chianelli, R. R.; Liang, K. S. *Surf. Sci.* **1984**, *140*, 181−196.
(5) Strongin, D. R.; Carrazza, J.; Bare, S. R.; Somorjai, G. A. *J. Catal.* **1987**, *103*, 213−215.
(6) Wakayama, H.; Setoyama, N.; Fukushima, Y. *Adv. Mater.* **2003**, *15*, 742−745.
(7) Lensveld, D. J.; Mesu, J. G.; van Dillen, A. J.; de Jong, K. P. *Stud. Surf. Sci. Catal.* **2002**, *143*, 647−657.
(8) Zong, Y.; Watkins, J. J. *Chem. Mater.* **2005**, *17*, 560−565.
(9) Singh, U. K.; Albert Vannice, M. *J. Catal.* **2000**, *191*, 165−180.
(10) Haran, N. P.; Bhagade, S. S.; Nageshwar, G. D. *Chem. Petro-Chem. J.* **1978**, *9*, 21−28.
(11) Hayek, K.; Goller, H.; Penner, S.; Rupprechter, G.; Zimmermann, C. *Catal. Lett.* **2004**, *92*, 1−9.
(12) Serp, P.; Hierso, J. C.; Feurer, R.; Kihn, Y.; Kalck, P.; Faria, J. L.; Aksoylu, A. E.; Pacheco, A. M. T.; Figueiredo, J. L. *Carbon* **1999**, *37*, 527−530.
(13) Chu, H. P.; Lei, L.; Hu, X.; Yue, P.-L. *Energy Fuels* **1998**, *12*, 1108−1113.
(14) Konya, Z.; Puntes, V. F.; Kiricsi, I.; Zhu, J.; Alivisatos, P.; Somorjai, G. A. *Catal. Lett.* **2002**, *81*, 137−140.
(15) Konya, Z.; Puntes, V. F.; Kiricsi, I.; Zhu, J.; Ager, J. W., III; Ko, M. K.; Frei, H.; Alivisatos, P.; Somorjai, G. A. *Chem. Mater.* **2003**, *15*, 1242−1248.

10.1021/cm0616681 CCC: $33.50
Published on Web 12/19/2006

substrate during the reaction, leading to destabilization of the nanocrystals. Furthermore, the surfactant templates used for the mesoporous material may interact with the nanocrystal surfaces and modify their morphologies.

An alternative approach is to decouple nanocrystal synthesis from the synthesis of the mesoporous material.[16,17] An advantage of this approach is that a large number of well-known synthetic methods may be utilized for the design of the nanocrystals[18] and of the mesoporous materials.[19] Prior to infusion, the particles are easily isolated from unwanted byproducts, cleaned, and separated by size, and the ligands may be exchanged, if desired, for alternative ligands. Here, it is not necessary to remove excess nanocrystal precursors and reaction byproducts from the pores as in traditional techniques such as wet impregnation.[20] After synthesis and purification, the nanocrystals may be infused into the pores of a presynthesized mesoporous material by a physical technique without modifying the structure of either material.

Rioux et al.[16] infused platinum nanocrystals coated with polyvinylpyrrolidone in an aqueous dispersion into high-surface-area mesoporous silica. Under sonication, pore loadings reached approximately 1 wt %. Without sonication, the nanocrystals were not able to infuse into the pores and remained coated on the outside of the silica. The nanocrystals penetrated the pores for a 1:1 mixture of water and ethanol, but not with pure water. The observed difference in penetration of the pores was attributed to the difference in surface tensions of water and ethanol.

In our previous study,[17] gold nanocrystals coated with dodecanethiol were infused into mesoporous silica to achieve highly dispersed nanocrystals with loadings greater than 2 wt %. The infusion required the addition of supercritical CO_2. CO_2 has a low polarizability relative to hydrocarbon solvents and serves as an antisolvent for the alkyl-coated nanocrystals.[21−23] (However, nanocrystal dispersions have been obtained in pure CO_2 at high temperatures[24] and in very dilute dispersions.[25]) For toluene expanded with CO_2, it is possible to tune the solvent strength to raise the long-ranged van der Waals interactions of the nanocrystals with the pore walls, and thus the nanocrystal loading, without flocculating the nanocrystals in the solution phase.[17] This goal was not achieved by adding methanol as an antisolvent to toluene.

The exact location of nanocrystals within the mesopores versus on the external surface is an important issue in metal/mesoporous silica catalysts. Rioux et al.[16] showed that nanoparticles, upon annealing at 400 °C, formed nanorods with a conformation related to the geometry of the cylindrical mesopores. However, the possibility of nanoparticles on the outside surface was not ruled out. To the best of our knowledge, the location of presynthesized nanocrystals infused into mesoporous materials has not been determined conclusively in previous studies. Midgley et al.[26] showed that the exact location of nanocrystals within mesoporous silica can be determined by Z-contrast scanning transmission electron microscopy (STEM) with a high angle annular dark field (HAADF) detector. The nanocrystals were synthesized inside the mesoporous silica by thermal reduction of a precursor. The use of a HAADF detector has the advantage that the images do not suffer from diffraction contrast. Furthermore, the contrast between heavy and light elements is enhanced, as the signal is proportional to the square of the atomic number.[27]

In a recent study of Pt nanocrystals infused into mesoporous silica,[16] the as-synthesized supported catalyst was inactive because the strongly bound polymeric shell blocked the active sites on the metal surface.[28] Calcination at 450 °C and above for 12 h was necessary to remove the polymeric coating and activate the catalyst. High-temperature annealing can potentially result in oxidation of the nanocrystals, can significantly change the nanocrystal size and surface morphology, and can also result in aggregation and coalescence, which reduces the available surface area of the catalyst.[29] The nature of ligand binding also has a large effect on homogeneous catalysis with nanoparticle solutions. Stowell et al.[30] showed that the catalytic activity of Ir nanocrystals in solution for hydrogenation of 1-decene was influenced markedly by the nature of the binding of the stabilizing ligands. Strong binding ligands passivated the surface and inhibited catalytic activity, while nanocrystals with weakly bound ligands showed much greater catalytic activity. However, as weakly bound ligands desorbed from the nanocrystals surface into the solvent, the nanocrystals aggregated and the activity declined.

Herein, we show that presynthesized iridium nanocrystals stabilized by weakly bound tetraoctylammonium bromide (TOAB) ligands may be infused into presynthesized mesoporous silica to produce a highly active catalyst for 1-decene hydrogenation. Z-contrast STEM with an HAADF detector is used to discriminate between nanocrystals within the mesopores and on the external silica surface. We chose to study decene hydrogenation, given the previous data for homogeneous catalysis with Ir nanocrystals in solution stabilized by TOAB.[30] The activity is compared for the original infused catalyst without pretreatment and for catalysts in which the ligands were removed by annealing at high temperature in air and nitrogen, or by extraction with

(16) Rioux, R. M.; Song, H.; Hoefelmeyer, J. D.; Yang, P.; Somorjai, G. A. *J. Phys. Chem. B* **2005**, *109*, 2192−2202.
(17) Gupta, G.; Shah, P. S.; Zhang, X.; Saunders, A. E.; Korgel, B. A.; Johnston, K. P. *Chem. Mater.* **2005**, *17*, 6728−6738.
(18) Yin, Y.; Alivisatos, A. P. *Nature* **2005**, *437*, 664−670.
(19) de Soler-Illia, G. J.; Sanchez, C.; Lebeau, B.; Patarin, J. *Chem. Rev.* **2002**, *102*, 4093−4138.
(20) Shyue, J.-J.; De, Guire, M. R. *J. Am. Chem. Soc.* **2005**, *127*, 12736−12742.
(21) Shah, P. S.; Holmes, J. D.; Doty, R. C.; Johnston, K. P.; Korgel, B. A. *J. Am. Chem. Soc.* **2000**, *122*, 4245−4246.
(22) Shah, P. S.; Husain, S.; Johnston, K. P.; Korgel, B. A. *J. Phys. Chem. B* **2001**, *105*, 9433−9440.
(23) Shah, P. S.; Husain, S.; Johnston, K. P.; Korgel, B. A. *J. Phys. Chem. B* **2002**, *106*, 12178−12185.
(24) Lu, X.; Ziegler, K. J.; Ghezelbash, A.; Johnston, K. P.; Korgel, B. A. *Nano Lett.* **2004**, *4*, 969−974.
(25) Bell, P. W.; Anand, M.; Fan, X.; Enick, R. M.; Roberts, C. B. *Langmuir* **2005**, *21*, 11608−11613.
(26) Midgley, P. A.; Weyland, M.; Thomas, J. M.; Johnson, B. F. G. *Chem. Commun.* **2001**, 907−908.
(27) Midgley, P. A.; Weyland, M. *Ultramicroscopy* **2003**, *96*, 413−431.
(28) Yoo, J. W.; Hathcock, D. J.; El-Sayed, M. A. *J. Catal.* **2003**, *214*, 1−7.
(29) Scott, R. W. J.; Wilson, O. M.; Crooks, R. M. *Chem. Mater.* **2004**, *16*, 5682−5688.
(30) Stowell, C. A.; Korgel, B. A. *Nano Lett.* **2005**, *5*, 1203−1207.

compressed carbon dioxide. The objective was to identify a ligand with sufficiently weak binding to the surface, such that it becomes unnecessary to pretreat the catalyst to remove the ligand.To prevent aggregation of the nanocrystals in solution during infusion, we added excess ligand to the solution. The effect of CO_2 concentration on the stability of the nanocrystal dispersion was investigated to identify the optimum conditions for the infusion. The stability of the catalyst was investigated by recovering the catalyst and performing a second reaction. The activation energy of the decene hydrogenation reaction was determined over a temperature range of 40−75 °C. The catalytic activities of the Ir nanocrystals infused into the mesoporous silica supports were compared with a commercial Pd hydrogenation catalyst supported on alumina used under the same reaction conditions.

Experimental Section

All chemicals were used as received. Tetraoctylammonium bromide or TOAB ($C_{32}H_{68}N$ Br, 98%), decane (99%), 1-decene (94%), and 1,2 hexadecanediol (90%) were purchased from Aldrich. (Methylcyclopentadienyl)(1,5-cyclooctadiene)iridium ((C_6H_7)(C_8H_{12})-Ir, 99%) was purchased from Strem. Toluene (99.9%) and concentrated liquid HCl (normality 12.1) were obtained from Fisher Scientific. Ethanol (Absolute 200 proof) was obtained from Aaper alcohol. Methanol (purity >99.8%) was obtained from EM Sciences. Tetraethoxysilane (TEOS) and dioctylether (97%) were obtained from Fluka Chemika and Poly(ethylene oxide)-*b*-poly-(propylene oxide)-*b*-poly(ethylene oxide) $EO_{\sim 20}PO_{\sim 70}EO_{\sim 20}$ (Pluronic P-123) from BASF Corporation. CO_2 (purity >99.99%; Matheson Gas Products) was used as received. Polycarbonate filters (0.05 μm) were obtained from Osmonics. Five percent palladium on alumina (Pd−Al_2O_3) commercial catalyst was obtained from Alfa Aesar. Water was doubly distilled and deionized.

Iridium Nanocrystal Synthesis. Iridium nanocrystals with TOAB ligands were synthesized by a method developed by Stowell et al.[30] using a 25 mL three-neck, round-bottom flask. Hexadecanediol (0.2 g), 7 mL of dioctylether, 0.2 g of (methylcyclopentadienyl)(1,5-cyclooctadiene)iridium, and 0.76 g of TOAB were measured into the flask. The solution was freeze−pump−thawed for three cycles using liquid nitrogen and heated to 270 °C for 30 min. The product was a black liquid, and the particles were isolated using one rinse in ethanol as an antisolvent. Rinsing the solution multiple times in ethanol resulted in the removal of capping ligands from the iridium surface,[30] so exposure to ethanol was kept at a minimum. The nanocrystals were finally dispersed in toluene before the infusion procedure. Excess TOAB ligand (10 mg/mL) was dissolved in the nanocrystal dispersion so as to prevent desorption of the ligands and hence prevent aggregation of the particles.

Mesoporous Silica Synthesis. Mesoporous silica SBA-15 (referred to as MPS) was synthesized with a block copolymer template similar to the reported procedure of Zhao et al.[31,32] A solution of 1.6 g of $EO_{20}PO_{70}EO_{20}$, 7 mL of HCl, 8 mL of TEOS, and 38 mL of H_2O was prepared, stirred for 24 h at 50 °C, and then heated at 100 °C for 24 h. The resulting slightly yellow powder was dispersed in ethanol, filtered, and then again heated at 100 °C for 24 h. Calcination was carried out by slowly increasing temperature from room temperature to 500 °C in 4 h and heating at 500 °C for 6 h.

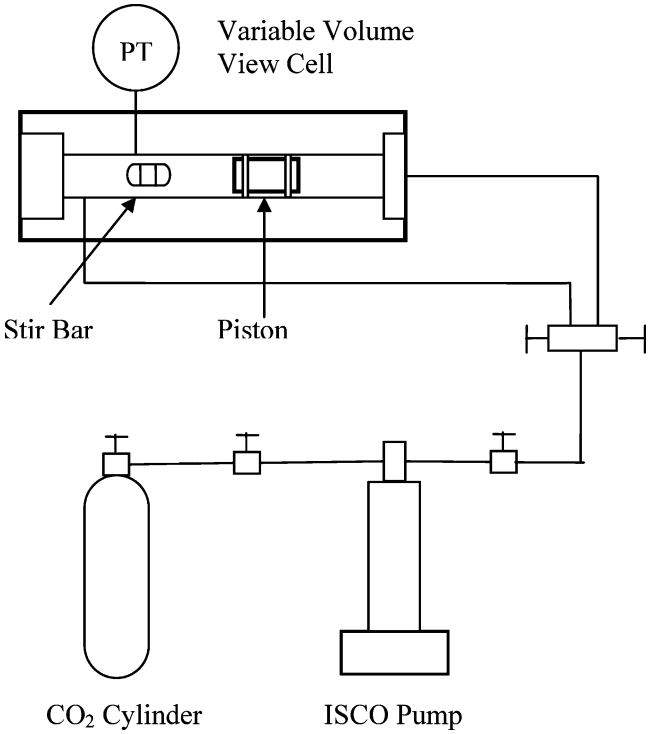

Figure 1. Schematic of the infusion apparatus.

Infusion of Ir into Mesoporous Silica with CO_2 as an Antisolvent. In a typical experiment, 100 mg of mesoporous silica and 6 mL of iridium nanocrystals dispersed in toluene, with a concentration of 0.4 mg/mL, were loaded into a variable-volume reaction cell[17] with a working volume (volume with piston in the cell) of 27 mL. An amount of CO_2 equivalent to 4 mL at 241 bar (3500 psia) and 35 °C was added so as to produce a 10 mL total volume of the reaction mixture. The cell was then pressurized to 241 bar with CO_2 at the back side of the piston using an ISCO model 100 DX computer-controlled syringe pump. The contents of the cell, in a water bath, were stirred with a magnetic stir bar (Figure 1). The reaction was maintained at 35 °C and 241 bar (3500 psia) and allowed to proceed for 24 h. After the reaction, the cell was cooled to 0 °C; CO_2 was then vented as a vapor from the top of the cell at the vapor pressure, 35 bar. The concentrations of organics in the CO_2 vapor were small at 0 °C such that losses were minimized. The supernatant was collected and filtered, using a polycarbonate 0.05 μm filter, to separate the Ir−MPS. Ir−MPS was cleaned by washing with 2 mL of pure toluene to remove the nanocrystals adsorbed on the outer surface of the silica. Hence the resulting nanocomposite contained Ir nanocrystals immobilized within the pores.

The extent of incorporation of iridium nanocrystals in the silica was determined by subtracting from the initial mass of the dispersed nanocrystals in toluene, the final mass of the nanocrystals recovered in the supernatant after filtration.[17] A correction was not made for the nanocrystals removed by washing with pure toluene. The absorbance of the iridium nanocrystals dispersed in toluene before and after infusion was measured at a wavelength of 500 nm using a Cary 500 UV−vis−NIR spectrophotometer with an optical path length of 1 cm. A standard calibration curve was generated at 500 nm using known concentrations of iridium nanocrystals in toluene, as shown in Figure 2. The experiments were repeated several times

(31) Zhao, D.; Feng, J.; Huo, Q.; Melosh, N.; Frederickson, G. H.; Chmelka, B. F.; Stucky, G. D. *Science* **1998**, *279*, 548−552.
(32) Zhao, D.; Huo, Q.; Feng, J.; Chmelka, B. F.; Stucky, G. D. *J. Am. Chem. Soc.* **1998**, *120*, 6024−6036.

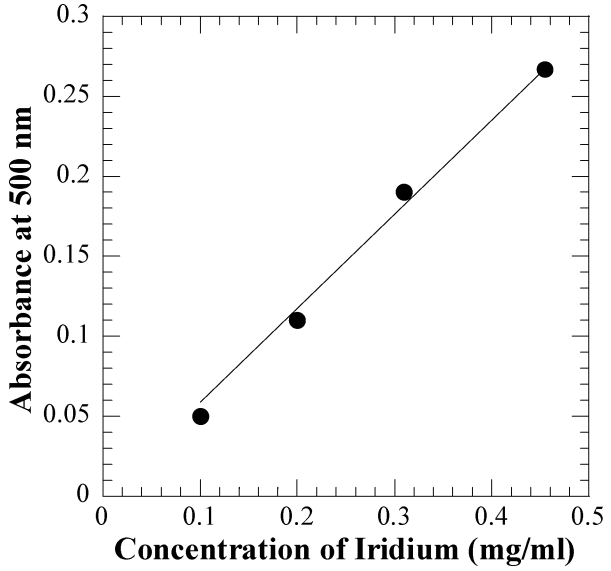

Figure 2. Calibration curve of UV−vis absorbance vs concentration for iridium nanocrystal dispersions in toluene, measured at 500 nm.

to check for the reproducibility in the nanocrystal loading, which was on the order of ±0.2 in wt % units, or 15% of the final Ir mass. The factors that cause uncertainty in final iridium loadings are volume measurement (1%), weight of silica (1%), uncertainty in absorbance (1%), and uncertainty in linearity (2−3%) of the calibration curve. Total uncertainty in loadings is reported as the sum of the uncertainty due to each individual factor, which is approximately 12%. The uncertainty in this method of loading determination is comparable to that of elemental analysis (10% error), which makes it equally effective for estimating the metal loadings. The concentration of nanocrystals washed from the outer surface of the silica with pure toluene was measured spectrophotometrically. The absorbance measured was less than 0.01 and within the detection limit, indicating a maximum of 0.1 mg of nanocrystals. The low concentration of nanocrystals is consistent with a ratio of external to internal surface area of mesoporous silica on the order of 1×10^{-4} on the basis of the pore diameter (∼1 nm) and particle size (∼10 μm). Hence, if the loading of nanocrystals is uniform on external and internal areas, then the loading on the external surface would be negligible (∼1×10^{-4}%).

Determination of Nanocrystal Precipitation Boundary. The effect of CO_2 concentration on the stability of the nanocrystal dispersions in the mixed solvent with toluene was determined. Nanocrystal dispersions were analyzed at 35 °C and 241 bar with a Cary 3E UV−vis spectrophotometer in a vertically mounted variable-volume high-pressure optical cell with a path length of 2 cm as described previously.[33] The schematic is shown in the Figure 3. Six milliliters of a 0.4 mg/mL concentration of iridium nanocrystals in toluene with 10 mg/mL excess ligands in the solvent was loaded in the front part of the cell. The contents were stirred using a magnetic stir bar. The computer-controlled ISCO syringe pump was used to introduce a known amount of CO_2 in the front part of the cell, and the cell was stirred for 30 s to mix the solvents. The stirring was stopped to allow the particles to settle, and the absorbance was measured for 20 min. Another aliquot of CO_2 was added and the procedure was repeated.

Catalysis. 1-Decene hydrogenation reactions were carried out in a 25 mL round-bottom flask batch reactor. Supported iridium nanocrystals were added to neat 1-decene to create a 1500:1 decene:

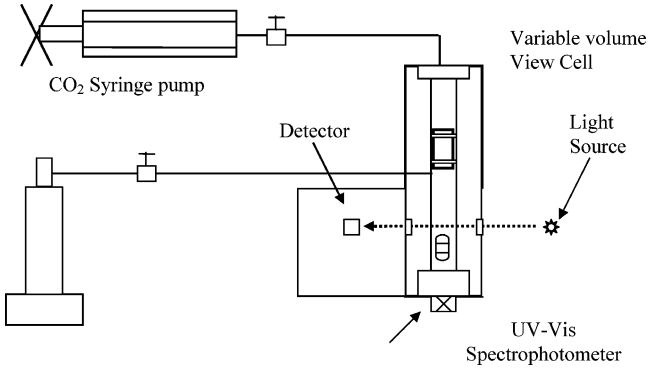

Figure 3. Schematic of apparatus for determining the dispersibility of the iridium nanocrystals in CO_2−toluene solvent.

iridium mass ratio. Hydrogen gas at 5 psig was bubbled into the dispersion. The system was stirred using a magnetic stir bar at high speed to raise mass-transfer rates. After the system was well-saturated with hydrogen for 20 min at 23 °C, the temperature was increased to the reaction temperature of 75 °C, and hydrogen flow was maintained throughout the reaction. Aliquots of the solution (100 μL) were removed every hour for the next 4 h and stored at room temperature in sealed vials for a maximum of 4 h before analysis by gas chromatography.

Characterization

Nitrogen Porosimetry. N_2 porosimetry was used to measure the surface area and the pore size distribution of the mesoporous silica with a high-speed surface area BET analyzer (NOVA 2000, Quantachrome Instruments, Boynton Beach, FL) at a temperature of 77 K. Silica samples were pretreated at 100 °C for 24 h in a vacuum immediately prior to data collection. Pore size distributions were analyzed using the adsorption branch of the isotherm. The Barrett−Joyner−Halenda (BJH) method[34] was used for pore size distribution.

Transmission Emission Microscopy. Low-resolution pictures of mesoporous silica, infused with iridium nanocrystals, were visualized by TEM on a Phillips EM280 microscope with a 4.5 Å point-to-point resolution operated with an 80 kV accelerating voltage. High-resolution transmission electron microscopy (HRTEM) was performed using a JEOL 2010F TEM operating at 200 kV. Z-contrast STEM was performed on FEI TECNAI G2 F20 X-TWIN transmission electron microscope using a HAADF (high-angle annular dark field) STEM detector with a 2 Å point-to-point resolution. Images were obtained primarily with a GATAN digital photography system. Silica particles were deposited from a dilute chloroform solution onto 200 mesh carbon-coated copper TEM grids (Electron Microscopy Sciences).

Gas Chromatography/ Mass Spectroscopy. The extent of catalytic conversion of 1-decene was determined with a Finnigan MAT GCQ gas chromatograph with mass spectrometer detector (GC/MS). The column used was DB5-MS (5% phenyl-methylpolysiloxane, J & W scientific) with a diameter of 0.32 mm and a length of 30 m. The GC was used in positive electron ionization mode with electrons accelerated at 70 eV. One-tenth of a microliter of the undiluted sample was injected using a split injection tech-

(33) Ryoo, W.; Webber, S. E.; Johnston, K. P. *Ind. Eng. Chem. Res.* **2003**, *42*, 6348−6358.

(34) Barrett, E. P.; Joyner, L. G.; Halenda, P. P. *J. Am. Chem. Soc.* **1951**, *73*, 373−380.

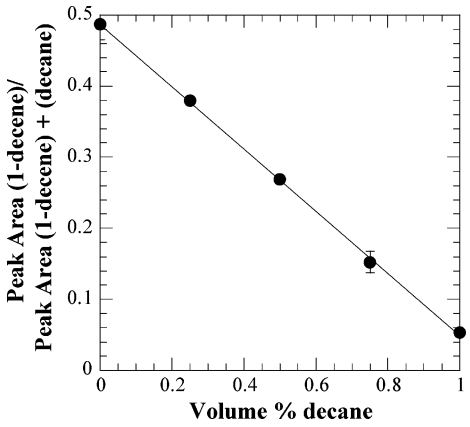

Figure 4. GC-MS calibration curve of a mixture of 1-decene and 1-decane.

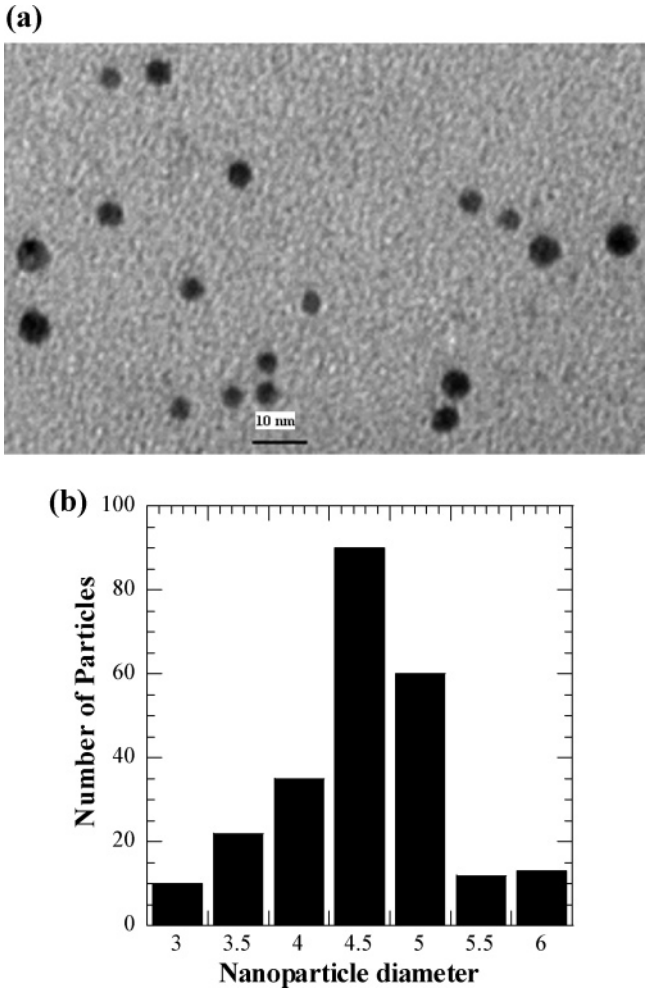

Figure 5. (a) TEM micrograph of iridium nanocrystals stabilized by TOAB and (b) corresponding histogram for iridium nanocrystals.

nique with an autosampler. The retention time of the 1-decene and decane peaks was approximately 30 s. The GCMS was calibrated to determine the relative amounts of 1-decene (MW = 140) and decane (MW = 142) in each aliquot, as shown in Figure 4. The curve was highly linear with a correlation coefficient of 0.9995.

Results and Discussion

Nanoparticle Characterization. Figure 5a shows a representative TEM image of TOAB-stabilized Ir nanocrystals.

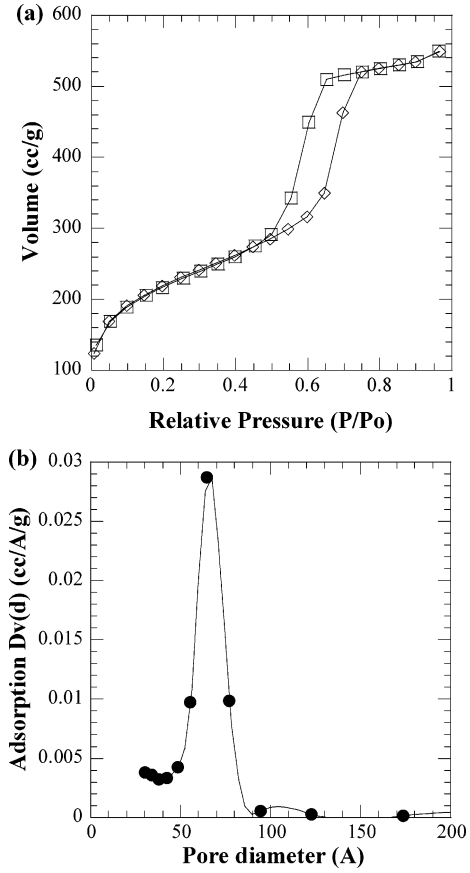

Figure 6. (a) N_2 adsorption−desorption isotherms for mesoporous silica MPS and (b) corresponding pore size distributions for MPS.

The particles were spherical in shape. By counting more than 200 particles, the average diameter was found to be 4.5 nm with a standard deviation of 0.6 nm (see Figure 5b). Nanoparticles in the image appear slightly larger than the original because of pixel aberration caused by image magnification.

Characterization of Mesoporous Silica. Representative nitrogen adsorption/desorption isotherms and corresponding pore size distributions (BJH method[34]) are shown in Figure 6. MPS has a mean pore diameter of 6.5 nm, BET surface area of 742 m^2/g and a pore volume of 0.98 cm^3/g. As well-cited in the literature for type SBA-15 mesoporous silica,[31] three distinct regions are evident in the adsorption isotherm: (i) monolayer−multilayer adsorption, (ii) capillary condensation, and (iii) multilayer adsorption on the outer particle surfaces. As can be seen in Figure 6, MPS shows a type-H1 hysteresis loop with capillary condensation at an activity $P/P_o = 0.7$.[31] The step in the hysteresis loop is very steep, with a jump from 300 to 500 cm^3/g, indicating capillary condensation. The slope and the height of the step are clear indications of very well defined mesopores with narrow pore size distribution.[35] In our previous study,[17] we measured interpore spacing of mesoporous silica type SBA-15 synthesized exactly as in the current study, using small-angle X-ray scattering (SAXS). SAXS showed multiple peaks, indicating a long range arrangement of pores with a pore diameter of 8.8 nm and a wall thickness of 3.1 nm, typically associated with SBA-15 silica.[31]

(35) Tanev, P. T.; Pinnavaia, T. J. *Chem. Mater.* **1996**, *8*, 2068−2079.

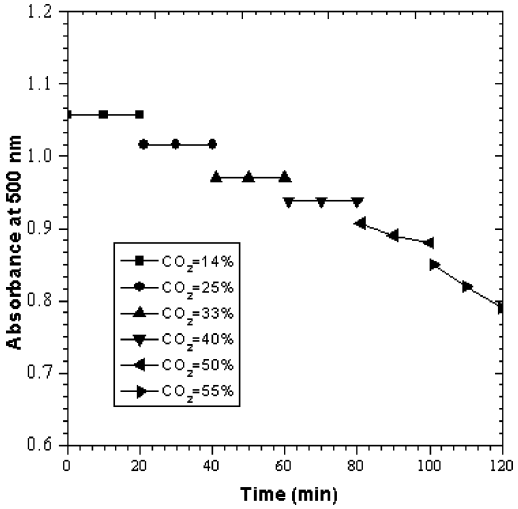

Figure 7. Dispersibility of Ir−TOAB nanocrystals in CO_2−toluene mixed solvent measured by UV−vis spectroscopy.

Nanocrystal Dispersibility in Toluene and Toluene−CO_2 Mixtures. The nanocrystals are stabilized in the dispersion by steric repulsion from the ligands adsorbed to the surface. The interactions between the ammonium bromide head group and metal surfaces like iridium[30] and gold[36] have been found to be relatively weak. For Ir, weak adsorption of TOAB ligands results in visible aggregation of the nanocrystals over a period of 12 h. Ligand desorption can be reduced by adding excess free ligand to the solvent. Mattoussi et al.[37] examined this concept quantitatively with SAXS studies on CdSe nanocrystals stabilized by trioctylphosphine and trioctylphosphine oxide (TOP/TOPO) dispersed in hexane. In the case of pure solvent with no excess ligands, the nanocrystals exhibited attractive interactions. However, the addition of free ligands eliminated interparticle attractions, and the nanocrystal interactions eventually became repulsive. In this study, ∼10 mg/mL TOAB was added to the Ir nanocrystal dispersion in toluene with a concentration of 0.5 mg/mL, and nanocrystals were found to be stable for several days on the basis of visual observation.

Figure 7 shows the absorbance at 500 nm of the Ir nanocrystal dispersion as a function of solvent composition and time. As the total amount of nanocrystals loaded in the variable-volume cell remains constant, the absorbance decreases as the concentration of Ir is decreased by the addition of CO_2 to the dispersion. It was determined that the absorbance remained constant with time for less than 50% CO_2 (w/w). When the CO_2 concentration reached 50%, the absorbance began to decrease modestly with time. At 55% CO_2, absorbance decreased faster, indicating faster aggregation and settling of particles. CO_2 is a poor solvent for the hydrocarbon ligands, and the insufficiently solvated ligands do not provide enough steric stabilization to counter the attractive van der Waals forces between the cores. Because large particles possess greater interparticle van der Waals attractions, they precipitate first upon the solvent quality being lowered.[38] On the basis of these results, the loading of the Ir particles for catalytic studies was performed at 40% CO_2, where the absorption was constant, indicating a stable dispersion.

Nanocrystal Loading in Pores using CO_2. The Ir nanocrystals dispersed in toluene−CO_2 solvent were infused into the mesoporous silica over a 24 h period. In our previous study,[17] we showed that 24 h was sufficient for reaching a maximum loading, with little increase from 24 to 72 h. We assumed 24 h was also sufficient in the current study, because the metal cores in each study had nearly the same Hamaker constants (gold vs iridium) and both studies used hydrocarbon ligands. The loading of the iridium nanocrystals within the mesoporous silica measured spectrophotometrically was about 1.3 ± 0.2 wt % (g of Ir/g of silica) for a CO_2 concentration of 40%. For the nanocrystals dispersed in pure toluene without CO_2, the loading was negligible. The high loading suggests that the nanocrystals are mobile on the silica pore surface, with the ability to diffuse deeply into the pores without causing pore blockage.

The equilibrium adsorption of a nanocrystal onto the silica surface within a pore is a function of the chemical potential of the nanocrystals in the solvent and the long-ranged van der Waals forces between the nanocrystals and silica surface, mediated by the intervening solvent.[17] The van der Waals force of attraction between the particle and the silica wall is directly proportional to the Hamaker constant of the system, A_{132}, for an iridium particle (1) and silica surface (2) across an intervening medium (toluene or toluene−CO_2 mixture, 3). It may be approximated by[39]

$$A_{132} = (\sqrt{A_{11}} - \sqrt{A_{33}})(\sqrt{A_{22}} - \sqrt{A_{33}}) \qquad (1)$$

where A_{ii} is the Hamaker constant for pure i, which can be estimated using a simplification of the Lifshift theory.[39]

$$A_{yy} = \frac{3}{4}k_b T\left(\frac{\epsilon_y - \epsilon_{vacuum}}{\epsilon_y + \epsilon_{vacuum}}\right)^2 + \frac{3h\nu_e}{16\sqrt{2}}\frac{(n_y^2 - n_{vacuum}^2)^2}{(n_y^2 + n_{vacuum}^2)^{3/2}} \qquad (2)$$

where ν_e is the maximum electronic ultraviolet adsorption frequency, typically assumed to be 3×10^{15} s^{-1}.[23] The A for iridium, 4×10^{-19} J,[39] the ϵ and n for silica, 3.91 and 1.45, respectively,[40,41] and for toluene, 2.38 and 1.496, respectively,[42,43] were taken from the literature. The Hamaker constants for silica and toluene calculated from eq 2 are 5.97×10^{-20} J and 6.98×10^{-20} J, respectively.

For pure toluene without CO_2, A_{132} is -0.31×10^{-20} J. The negative sign in the overall Hamaker constant indicates that the interactions between the iridium nanoparticle and

(36) Saunders, A. E.; Sigman, M. B., Jr.; Korgel, B. A. *J. Phys. Chem. B* **2004**, *108*, 193−199.
(37) Mattoussi, H.; Cumming, A. W.; Murray, C. B.; Bawendi, M. G.; Ober, R. *Phys. Rev. B: Condens. Matter Mate. Phys.* **1998**, *58*, 7850−7863.
(38) McLeod, M. C.; Anand, M.; Kitchens, C. L.; Roberts, C. B. *Nano Lett.* **2005**, *5*, 461−465.
(39) Israelachvili, J. *Intermolecular & Surface Forces*, 2nd ed.; Academic Press, Inc.: San Diego, 1992.
(40) Hourri, A.; St-Arnaud, J. M.; Bose, T. K. *J. Chem. Phys.* **1997**, *106*, 1780−1785.
(41) Burns, R. C.; Graham, C.; Weller, A. R. M. *Mol. Phys.* **1986**, *59*, 41.
(42) Rubio, J. E. F.; Arsuaga, J. M.; Taravillo, M.; Baonza, V. G.; Caceres, M. *Exp. Therm. Fluid Sci.* **2004**, *28*, 887−891.
(43) Williams, J. W.; Krchma, I. J. *J. Am. Chem. Soc.* **1926**, *48*, 1888−1896.

the silica wall were repulsive or unfavorable for particle adsorption. Hence, even though the nanocrystals can diffuse inside the pores along with the solvent and fill the pores, the weak adsorption onto the silica surface may be expected to result in low loadings, as observed experimentally. If the dispersion of nanocrystals in the pores contained the bulk concentration of nanocrystals, the calculated loading would be less than 0.1 wt %, as the internal pore volume was only 1% of the entire volume in the system.

CO_2 has an unusually low polarizability/density (very weak vdW forces) and may be added to a liquid solvent to form a mixture with an unusually low Hamaker constant.[17] The Hamaker constant for pure CO_2 was calculated to be only 1.44×10^{-20} J.[17] The Hamaker constant of the intervening mixed-solvent A_{33} was determined for the binary solvent mixture with the Lorenz−Lorenz mixing rule, as described previously.[17] The interactions between the nanocrystals and silica become strongly attractive as the Hamaker force of the mixed solvent is reduced by adding CO_2.[17] For 40% CO_2 in the intervening solvent, A_{132} was determined to be 4.1×10^{-20} J, indicating strong attractive interactions of the Ir nanocrystals with the silica surface. The high Ir loading of 1.3 wt % seen experimentally was consistent with this prediction, as was the low loading for pure toluene, where A_{132} was weakly repulsive.

The low Hamaker constant of the mixed solvent, and the weaker solvation of the ligands, also strengthens the interactions between the nanocrystals in solution, as is seen in Figure 7. However, iridium nanocrystals form a stable dispersion with 40% CO_2 in the solvent mixture. Thus, the solvent strength may be tuned with CO_2 to achieve strong adsorption on the silica surface, and thus high loading of nanocrystals, without aggregating the nanocrystals in solution. The ability to fine-tune the solvent strength with CO_2 to achieve high nanocrystal loadings has also been observed for Au nanocrystals.[17] Given these results for gold, it is to be expected that Ir could also be infused into silica, given the similar Hamaker constants for Au and Ir and the similar hydrocarbon tails in the ligands used in both studies.

TEM Micrographs of Infused Silica. High-resolution Z-contrast STEM was utilized to confirm that most of the nanocrystals are dispersed within the pores, rather than on the external surface of the particles. The contrast variation in the STEM is proportional to the mass density of the region multiplied by the atomic number squared (Z).[27] Regions of high density are shown in white. Figure 8a shows the planar view of the nanocrystals aligned within the pores. Iridium has a higher atomic number and mass density with respect to the pore walls composed of silica, which in turn are denser than empty pores. Hence, the iridium nanocrystals are observed as spherical bright dots, silica walls appear as discrete white lines, and empty pores appear as dark spaces between the silica walls. Most of the nanocrystals are aligned within the empty pores along the pore wall, whereas a small fraction appears to be in the pore wall. The nanocrystals, which appear to be on the pore walls, could have been in many cases located inside the secondary pores (which act as interconnects between the pores) within the pore walls, which can be as large as 4 nm in diameter for mesoporous silica of type SBA-15.[44]

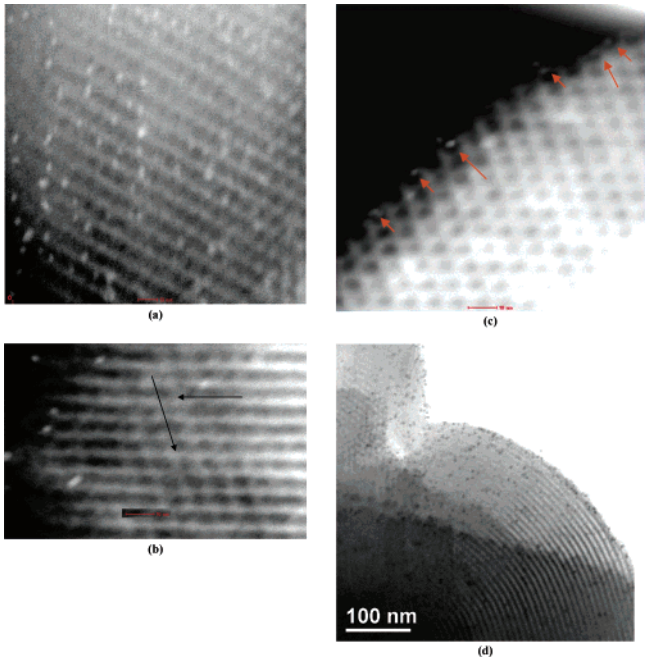

Figure 8. (a) Z contrast STEM (planar view) of MPS infused with Ir−TOAB; (b) out of focus view of (a); (c) top down view of (a); and (d) TEM micrograph of MPS infused with Ir−TOAB nanocrystals without any pretreatment. Scale bars in (a−c) are 10 nm.

Figure 8b is an out-of-focus image of 8a showing two different planes of ordered pores (as indicated by arrows) with iridium nanocrystals inside the pores. The planes were too close together to come from two different particles, but instead indicated a fault line in the surfactant template for a single particle. Thus these nanocrystals were in the interior of a particle in the pores and not on the surface, further supporting the observations in Figure 8a. Figure 8c shows the top down view of the pores, where we see the pore opening on the silica surface, with pores arranged in hexagonal assembly. The arrows indicate the nanocrystals that are located within the dark empty pores. Almost all the nanocrystals are dispersed within the pores rather than on the external surface, consistent with the much higher internal surface area as compared to the external area. The micrographs thus conclusively prove that almost all the iridium nanocrystals are present within the pores.

Further evidence that the nanocrystals are mostly within the mesopores is provided by the theoretical estimate of the close-packed monolayer coverage for nanocrystals on the external silica surface. The particle diameter was measured to be greater than 10 μm by laser light scattering (Malvern Mastersizer-S, Malvern Instruments Inc., Southborough, MA). The average molecular weight of 4.5 nm Ir nanocrystals was approximated to be about 400 000 g/mol. The external surface area of 10 μm nonporous silica spheres is 0.3 m^2/g. From geometrical calculations, it was found that in a hexagonal unit lattice, 45% of the surface area was occupied by pores. With this correction for 7 nm pores, the maximum external surface area of the porous silica particles was determined to be 0.16 m^2/g. In addition, the packing

(44) Joo, S. H.; Choi, S. J.; Oh, I.; Kwak, J.; Liu, Z.; Terasaki, O.; Ryoo, R. *Nature* **2001**, *414*, 470.

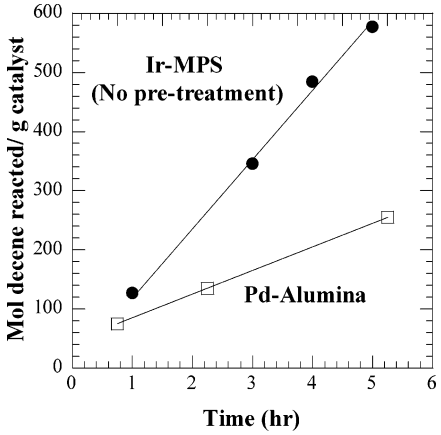

Figure 9. Comparison of catalyst activities for decene hydrogenation with Ir−MPS (without any pretreatment) and an industrial catalyst, Pd−Al_2O_3.

density of 0.906 (maximum density considering hexagonal close packing) was assumed for the monolayer assembly, which arises because of the voids between the spherical nanocrystals. The 1.3 wt % loading corresponded to 1.96×10^{16} nanocrystals per g of silica, whereas only 4.3×10^{15} nanocrystals were required for forming a close-packed monolayer on the external silica surface. The 1.3 wt % loading of nanocrystals was therefore approximately 4.5 times that of monolayer coverage on the external surface. Thus, even if external surface area was covered by a monolayer of iridium nanocrystals, 78% of the nanoparticles would still be inside the pores, consistent with the observations by Z-contrast microscopy. The high loading in the pores suggests that the adsorbed particles are mobile and can move toward the center of the pore by diffusion on the surface and/or in the bulk, without blocking the pores.

Figure 8d shows a typical HRTEM image (without Z contrast) of Ir nanocrystals infused into mesoporous silica. The nanocrystals are highly dispersed, although the resolution is considerably lower than in the Z contrast images in Figure 8a−c. Therefore, the Z contrast images are needed to demonstrate conclusively that the nanocrystals are in the pores.

Decene Hydrogenation on Ir/MPS Catalysts. The rates for 1-decene hydrogenation with uncalcined Ir/MPS are shown in Figure 9. The conversion was linear in time. As the reaction was conducted in 1-decene as a neat solvent, the reaction rate was zero order with respect to 1-decene. Given that the solvent was the reactant, the mass-transfer resistances for 1-decene to the surface were negligible. The surface of the catalyst was constantly saturated with 1-decene, eliminating any concentration dependence with time. The linearity also suggested that the catalyst was not deactivated over the course of the experiment. Hydrogen was continuously bubbled into the reaction mixture at 760 Torr to maintain a constant H_2 concentration in the liquid phase. The rate of 1-decene hydrogenation is a function of reaction temperature, concentration of hydrogen in the liquid phase, and the 1-decene concentration as follows

$$-r_{\text{decene}} = A\exp\left(\frac{-E_a}{RT}\right) f(C_{\text{decene}}, C_{H_2}) = \text{constant} \quad (3)$$

where A is the pre-exponential factor, E_a is the activation energy, C_{decene} is the concentration of neat 1-decene, and C_{H_2} is the concentration of dissolved hydrogen in the liquid phase. In our case, all three factors remain constant; hence, the rate of reaction remains constant.

A turnover frequency (TOF) can be defined as the moles of reactant consumed per unit time per mole of available active sites of the catalyst[30]

$$\text{TOF} = \left(\frac{1}{N_{\text{site}}}\right)\left(\frac{dm_{\text{decene}}}{dt}\right) \quad (4)$$

where $N_{\text{site}} = n(A_p/A_{\text{uc}})$, A_p is the surface area of the nanocrystal determined from TEM, A_{uc} is the area of one unit cell on the surface, and n is the number of Ir atoms in a unit-cell face. The number of surface unit cells is simply A_p/A_{uc}. The number of active sites may only be approximated. Even if the moles of binding sites are measured for a certain gas via chemisorption, the active sites for the catalytic reaction may not be exactly the same sites.[28] We chose to assume that the TOAB ligands did not block any active sites, as has been assumed in similar studies.[28,45] It was assumed that all of the surface Ir atoms were active, resulting in a conservative lower limit for the TOF via eq 4. The number of surface atoms was determined from the total surface area of the nanocrystals, the number of iridium unit cells on the surface, a lattice length of 0.384 nm, and the number of iridium atoms within the FCC unit cell.

Turnover Number for Uncalcined Ir−MPS. The TOF for uncalcined Ir−MPS in the 1-decene hydrogenation was 16 s^{-1}. The highly dispersed nanocrystals, with an average diameter of 4.5 nm and minimal aggregation, enabled the high catalyst activity. The use of weakly binding ligands for nanoparticle stabilization in the bulk solvent, which readily desorb from the surface of the Ir nanocrystals dispersed on the support, may be expected to produce a large number of active sites and thus high catalyst activity.

For metal nanocrystals with very high activities, it can be challenging to prevent poisoning of the surface during reaction resulting in reduced catalytic activity or, in some cases, complete deactivation.[28] Catalyst deactivation can be particularly severe for concentrated reactants, in our case, pure reactant.[46] To determine if Ir−MPS undergoes any surface poisoning during decene hydrogenation, the Ir−MPS was recovered and used for a second catalytic reaction. Table 1 illustrates that the activity dropped by only 7% in the second reaction, within experimental error, and remained much higher than the industrial catalyst in the first reaction.

Effect of Catalyst Pretreatment for Ligand Removal on Catalytic Activity. Although capping ligands are necessary for dispersing the nanocrystals during infusion, they potentially may have a negative effect on the catalytic activity if they block active sites on the Ir surface. Stowell et al.[30] showed that iridium nanocrystals stabilized with strongly bound ligands such as oleic acid/oleylamine were essentially catalytically inactive, whereas those stabilized with weakly bound ligands such as TOAB provided much higher catalytic

(45) Le Bars, J.; Specht, U.; Bradley, J. S.; Blackmond, D. G. *Langmuir* **1999**, *15*, 7621−7625.
(46) Ha, S.; Larsen, R.; Masel, R. I. *J. Power Sources* **2005**, *144*, 28−34.

Table 1. Activity and Turnover Frequency for Decene Hydrogenation of 1.3% Ir Supported on Mesoporous Silica Relative to 5% Pd on Alumina

catalyst	*T* (°C)	TOF (mol of decene reacted/mol of surface atoms of catalyst/s)	activity (mol of decene reacted/ g of metal/s × 10^4)
Ir−MPS (uncalcined)	75	16.3	1.66
Ir−MPS (second run uncalcined)	75	15.1	1.54
Ir−MPS (calcined in an inert atmosphere, nitrogen at 500 °C for 6 h)	75	15.4	1.59
Ir−MPS (annealed in CO_2 at 4000 psi, 60 °C for 12 h)	75	17.1	1.75
Ir−MPS (calcined at 250 °C for 6 h in air)	75	11	1.12
Ir−MPS(calcined at 500 °C for 6 h in air)	75	4	0.41
Ir−MPS (uncalcined)	50	5.7	0.58
Ir−MPS (uncalcined)	40	2.4	0.25
5% Pd on alumina (industrial catalyst)	75	−	0.92

activity. The TOF in decene hydrogenation improved significantly with successive reactions, from 5 s^{-1} to 124 s^{-1}, as the weakly bound ligands desorbed from the surface. However, the nanocrystals eventually aggregated from too much ligand desorption, resulting in a loss in surface-to-volume ratio and activity.[30] This aggregation may be mitigated by supporting the nanocrystals within mesoporous silica.

Table 1 compares the TOFs, with 760 Torr hydrogen pressure at 75 °C unless otherwise specified, for decene hydrogenation for Ir−MPS catalysts pretreated in various ways. The TOF obtained with the untreated Ir−MPS was 16 ± 1 s^{-1}. The TOF was essentially the same when the catalyst was calcined in an inert nitrogen atmosphere at 500 °C for 6 h. This temperature was sufficient to desorb and volatilize the TOAB ligands. The nanocrystals were immobilized on the support, as they did not show any deactivation from sintering upon calcination at 500 °C. The catalysts were also calcined in air at two different temperatures, 250 and 500 °C. The TOF decreased from 16.5 to 11 s^{-1} when calcined at 250 °C and to 4 s^{-1}, less than a quarter of the original activity, at 500 °C. Given that the TOF did not change after calcination in N_2 at 500 °C, the loss in activity upon calcination in air may be attributed to oxidation of the surface of the Ir nanocrystals. Annealing in supercritical CO_2 at 275 bar pressure and 60 °C for 12 h produced a slight increase in the catalytic activity. The solubility of the ionic molecule TOAB in supercritical CO_2 may be expected to be low and, hence, 0.1 g of 1.3% Ir−MPS was annealed in approximately 25 g of supercritical CO_2.

In the case of supported nanocrystals on mesoporous silica, we observe that high catalytic activity may be obtained without thermal pretreatment to remove the ligands from the surface. Furthermore, the high activity remains constant even after pretreatment by (a) thermal calcination in N_2 and (b) CO_2 extraction. Thus, any ligands on the surface prior to these pretreatments did not inhibit catalyst activity, as was the case for polymeric stabilizers on Pt nanocrystals.[28] Further evidence will be provided to explain this highly beneficial result.

The TOAB ligands will partition between the bulk phase, the nanocrystals, and the mesoporous silica during the infusion process and during the catalytic reaction. The mesoporous silica with a surface area of 742 m^2/g has a large number of sites for ligand adsorption. The total surface area of the adsorbed nanocrystals was only 3.5 m^2. Suppose that all of the TOAB adsorbed exclusively on the silica. The area for a linear dodecanethiol ligand has been reported to be approximately 20 A^2 per molecule.[47] If it is assumed that the area of TOAB (highly branched) is twice that of dodecanethiol, we estimate that the total amount of TOAB required for monolayer coverage on the mesoporous silica is about 1.7 g of TOAB/g of silica. Consequently, even if all the TOAB in the system (60 mg added) adsorbed exclusively on the mesoporous surface, only 35% of the silica sites would be covered. Thus, it is likely that a large fraction of the weakly bound ligands on the dilute nanocrystals within the pores will migrate to the vacant sites on the silica and reduce the coverage of ligands on the surface. Ligand desorption from the nanocrystals will increase the number of catalytically active sites.

TOAB's weak binding and highly branched architecture will leave more catalytic sites available relative to ligands such as oleic acid and oleylamine. The volume occupied by the small ammonium bromide head groups will be relatively small for TOAB relative to the larger volume of the four hydrocarbon tails. In essence, the bulky tails will leave gaps between the head groups containing active catalytic sites for the small hydrogen molecules. Consequently, H_2 atoms may still chemisorb on the surface and react very close to the binding site of the TOAB underneath the larger cone of the tail groups. The transfer of ligands from the nanocrystals to the silica surface and the gaps between the headgroups of the ligands is likely to play an important role in the high activity of the catalysts without pretreatment.

Stability of Supported Nanocrystals during the Reaction. It was determined that the metal nanocrystals do not desorb from the mesoporous silica upon exposure to the 1-decene during 4 h of reaction at 75 °C. After the reaction, the mixture was filtered and the supernatant was recovered and analyzed spectrophotometrically at 500 nm. The absorbance was below the detectable limit within the experimental uncertainty (<0.005). From an extrapolation of the calibration curve (Figure 10), the concentration of the desorbed iridium nanocrystals was determined to be less than 0.01 mg/mL, or less than 3% of the total amount of catalyst. The stability of the catalyst against nanocrystal desorption is further supported by the fact that the TOF for the second catalytic run was almost the same as that of the original run, as shown in Table 1. Figure 11 shows the TEM micrograph

(47) Korgel, B. A.; Fullam, S.; Connolly, S.; Fitzmaurice, D. *J. Phys. Chem. B* **1998**, *102*, 8379−8388.

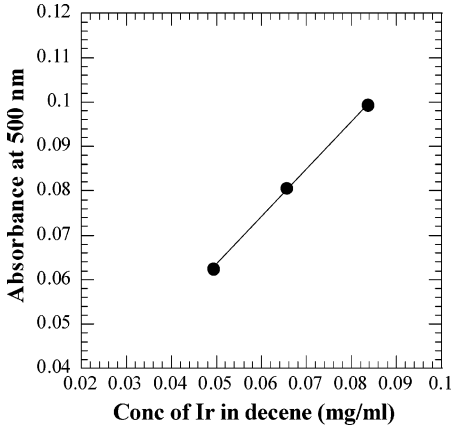

Figure 10. Calibration curve of UV−vis absorbance vs concentration for iridium nanocrystal dispersions in 1-decene, measured at 500 nm.

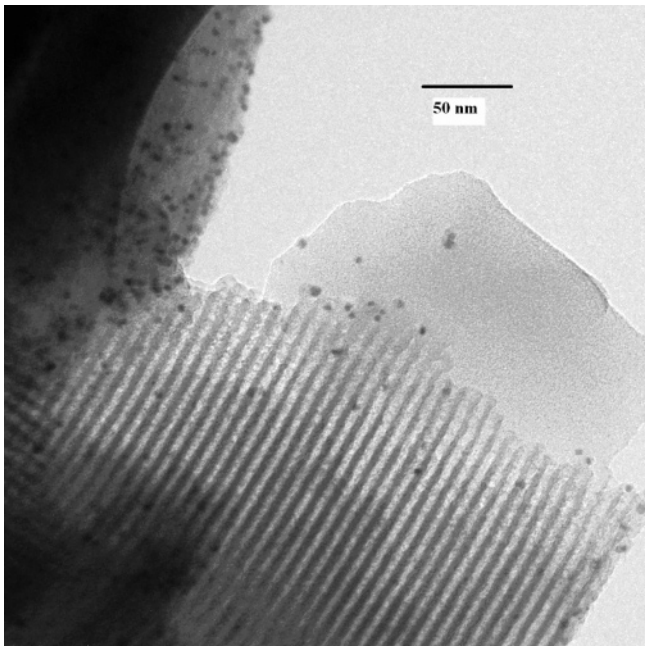

Figure 11. TEM micrographs of Ir−MPS (without any pretreatment) after 1-decene hydrogenation.

of Ir−MPS after reaction of 1-decene with hydrogen for 4 h. The micrograph shows that the particles were well-dispersed and did not aggregate, further indicating the stability of the nanocrystals within mesoporous silica. The expected desorption of the ligand from the adsorbed nanoparticle surface onto silica would increase the attractive van der Waals attraction between the particle and the silica, further enhancing its binding to the surface.

Activation Energy of the Decene Hydrogenation. The apparent activation energy for the decene hydrogenation by Ir−MPS was measured over a temperature range of 40−75 °C, as shown in Table 1. As shown in the Arrhenius plot for the TOF[16] (Figure 12), the activation energy was approximately 13.5 kcal/mol. To further put our results in perspective, the catalytic activity of Ir−MPS was compared with a typical industrial hydrogenation catalyst (5% palladium on alumina). Decene hydrogenation reactions were performed under identical conditions with the same mass of metal, as shown in Figure 9. The rate of decene hydrogenation is constant for Pd−alumina, as was observed above for Ir−MPS for the same reasons. For Ir−MPS, the activity was

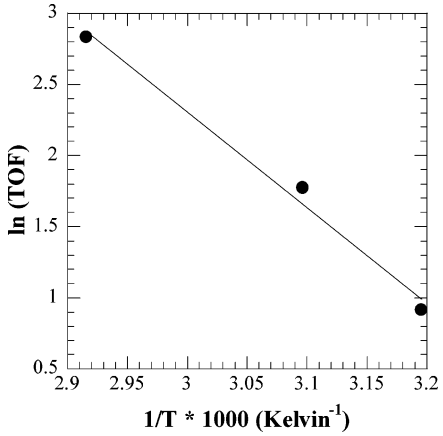

Figure 12. Arrhenius plot of decene hydrogenation over untreated Ir−MPS.

117 mol of decene reacted/g of Ir/h versus only 65 for Pd. For the Pd catalyzed reaction of 1-decene, the activation energy was 17 kcal/mol.[48] The higher activity for Ir−MPS vs Pd−alumina, by a factor of 1.8, is caused in part by the high surface area on the order of 80 nm^2 for 5 nm in diameter Ir nanocrystals. The greater fraction of surface atoms of metal, as characterized by the higher surface area, increases the number of active sites.

Conclusions

Herein, we show a novel approach for designing catalysts with high activities by infusing presynthesized iridium nanocrystals with well-defined surface morphologies into ordered mesoporous silica. Decoupling the synthesis step and the infusion step enables control of the iridium nanocrystal size, morphology, catalytic properties, and dispersibility within the mesopores. A dispersion of iridium nanocrystals may be infused into mesoporous silica by expanding the solvent, toluene, with supercritical CO_2. High loadings of the nanocrystals are achieved by tuning the solvent strength with CO_2, in order to strengthen the interactions of the nanocrystals with the pore walls, without flocculating the nanocrystals in the bulk solvent. With Z-contrast STEM using a HAADF detector, it was demonstrated clearly that the iridium nanocrystals are highly dispersed within the pores, with relatively few particles on the external particle surface. The ability to maintain the predesigned nanocrystal size during infusion and to achieve high loadings within the pores, as characterized by Z-contrast TEM, are important milestones in the development of highly active and selective catalysts. The high surface area of the nanocrystals produced high turnover frequencies (TOF) of 16 s^{-1} for decene hydrogenation, even without thermal pretreatment to remove the TOAB ligands. The TOF was higher than the initial TOF for homogeneous catalysis[30] with the same nanocrystals dissolved in 1-decene. Thermal calcination at 500 °C or CO_2 annealing at 275 bar had no impact on catalyst activity, which is not surprising, given the high activity of the original catalyst.

The nanocrystals remain dispersed in the pores and do not aggregate or desorb into the solvent during the reaction, as

(48) Goyal, H. B.; Gupta, A. K. *Indian J. Technol.* **1989**, *27*, 360−362.

observed by postreaction TEM and UV−vis spectrophotometric analysis of the product solution. Weakly bound ligands on the nanocrystal surface, such as TOAB, may be expected to migrate to the vacant sites on the silica, significantly reducing the ligand coverage on the surface and hence increasing the catalyst activity. Additionally, tetraoctylammonium bromide ligands with bulky tails will leave gaps between the head groups, allowing small hydrogen molecules to chemisorb on the surface and react very close to the binding site of the TOAB. Desorption of ligands from the adsorbed nanoparticle surface, onto the support and into the decene during reaction, will enhance metal binding to the surface and aid catalyst stability. This general infusion method for controlling the size, surface morphology, and stabilizing ligands of the nanocrystals, independently of the synthetic procedure for the mesoporous material, offers broad opportunities in designing novel highly active catalysts.

Acknowledgment. This material is based on work supported in part by the STC Program of the National Science Foundation under Agreement CHE-9876674, the Department of Energy Office of Basic Energy Sciences, the Robert A. Welch Foundation, and the Separations Research Program at the University of Texas.

CM0616681